Introduction

One of the most striking anatomical differences between the accessory and main olfactory bulbs in mammals is the dendritic morphology of the mitral cells. The vast majority of mitral cells in the main olfactory bulb have primary dendrites that form a single dendritic tuft occupying a single glomerulus, whereas most accessory olfactory bulb (AOB), most mitral cells are multi-tufted. The multitufted AOB mitral cells, like the multitufted mitral cells of other species (Meisami & Bhatnagar, 1998), seem to be designed to sample inputs from multiple glomeruli, which presumably are then integrated to generate somatic depolarization and mitral cell firing. We wish to understand the functional consequences of these multitufted mitral cells, starting with the question of whether they act in a linear or nonlinear fashion.

Methods:

Sagittal slices of mouse accessory olfactory bulb were prepared according to procedures similar to those described previously for cutting slices of the main olfactory bulb (Margrie *et al.*, 2001;Nickell *et al.*, 1994). Whole cell recordings from mitral cells were obtained using Multiclamp 700A amplifiers (Axon instruments, Foster City, CA), ITC-18 data acquisition boards (Instrutech, Port Washington, NY) and custom software written in Igor (Wavemetrics, Lake Oswego, OR). Cells were visualized using infrared differential interference contrast (DIC) optics (Olympus BX51WI, 60x 0.9 NA objective) and video microscopy (Dage/MTI). Prior to recording, slices were placed in a submersion chamber and perfused (at 1-2 ml/min) with oxygenated Ringer's solution maintained at 33-35 °C. Whole cell pipettes (3-7 MΩ) were pulled from borosilicate glass and filled with solutions containing (in mM): Potassium gluconate 130, HEPES 10, MgATP 2, GTP 0.3, biocytin 0.5-1%, and Alexa (either 594 or 488) hydrazide 0.01 at pH 7.3.

For calcium imaging experiments mitral cells were filled via the whole-cell recording pipette using an internal solution (above) containing 50-200 μM of a calcium orange. Images were acquired by a back-illuminated, cooled CCD camera (Princeton Instruments, Micromax CCD57

512 BFT) operated in the frame transfer mode and controlled by custom software written in Igor (Wavemetrics), using the SIDX camera control interface (Bruxton). Calcium transients are reported as $\Delta F/F$, after appropriate corrections for background fluorescence and bleaching have been made (Margrie *et al.*, 2001).

Extracellular stimulation electrodes were made from glass pipettes identical to those used for whole cell recordings. These electrodes were filled with oxygenated Ringer's solution and connected to one pole of the stimulus isolation unit (SIU; AMPI, Israel).

Cell morphologies obtained from the Neurolucida system were converted to **Neuron** *.hoc files using a JAVA-based program (CVAPP written by Robert Cannon of Edinburgh, UK). These detailed morphological data were imported into **Neuron** (Michael Hines, of Yale University) and used to simulate electrophysiological data. Simulations were run in **Neuron** on standard Pentium 4-based PCs. The passive properties of these neurons were chosen so that the behavior of the compartmental model approximates that of the real mitral cell. For these models, initial values for the passive parameters will be R_m = 10 KΩ-cm^2, R_a= 330 KΩ-cm, Cm = 1 μF/cm^2, V_{rest} = -60 mV.

Results:

We used compartmental models to examine passive signal transfer in the dendritic trees of AOB mitral cells. These models allow us to determine the degree to which AOB dendritic tufts are electrically isolated from each other and from the soma. The degree of electrical isolation can be determined by measuring the amplitude of voltage changes elicited by current injection at a given dendritic location both at the site of the injection and also at other locations in the dendrite (Spruston *et al.*, 1994). Because dendrites act as low pass filters (Segev & Parnas, 1983;Shepherd *et al.*, 1985), the amount of attenuation observed depends on the time course of the injected current, and thus the attenuation can be plotted as a function of the frequency of the input. Fast synaptic events with rise times of a few milliseconds (such as AMPA receptor-

mediated EPSPs) will be more strongly filtered than will slower depolarizations (such as those due to NMDA receptor mediated currents).

Our simulations show that the tufts of AOB dendritic trees are electrically quite remote from each other and from the mitral cell soma. The amount of attenuation varies with cell morphology and with the choice of passive parameters, but in the example shown in Figure 1 the attenuation of a simulated fast synaptic current between tuft and soma is >95%. The attenuation between two tufts in this same cell is similar to the attenuation between tuft and soma, although the exact value of the attenuation between tufts depends heavily on whether or not the tufts are part of the same primary dendritic arbor. The steady state attenuation from tuft to soma in the cell shown in Figure 2 is still >95%, suggesting that for input arriving at a tuft to have a substantial effect on somatic membrane potential may require propagation of regenerative events, such as action potentials in mitral cell primary dendrites.

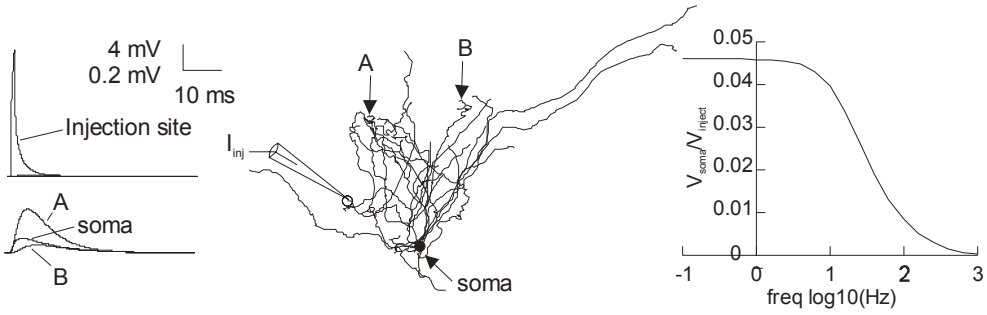

Figure 1: Passive attenuation of signals from tuft to soma and from tuft to tuft in AOM mitral cells. (Left) In this particular AOB mitral cell (middle), which had one of the more complex dendritic arborizations of the mitral cells that we have reconstructed, injection of a 1 ms current pulse results in a 40 mV depolarization at the site of current injection, but less than 1 mV of depolarization at the soma, or in any other tuft. Note, the tufts of this particular cell were very dense and individual dendritic branches could not be visualized clearly so the measurements are made from the primary dendrite at the base of the tuft. (Right) The attenuation of voltage propagating from the injection site to the soma is plotted against the log of the frequency of the injected current.

The dendrites of many neurons contain voltage-gated sodium or calcium channels that can support the propagation of action potentials. The extent of the propagation depends in part on the density of channels (Migliore & Shepherd, 2002), and in part on morphology (Schaefer *et al.*, 2003). Here we show that a single action potential, initiated by somatic current injection, results in a calcium elevation throughout the primary dendrites of AOB mitral cells, including the distal

tuft Figure 2B1, B2). The amplitude of the calcium transient measured in the tuft is similar to that recorded in the portions of the primary dendrite nearest to the soma (N=9 cells). These data suggest that somatically initiated action potentials propagate to the dendritic tufts of AOB mitral cells, as has been shown previously for mitral cells of the MOB (Chen *et al.*, 1997;Bischofberger & Jonas, 1997;Margrie *et al.*, 2001). Activation of dendritic voltage-dependent channels (including calcium channels) is a possible mechanism by which the dendrites may respond to synaptic input in a non-linear fashion and by which coincident activity of nearby inputs may be detected.

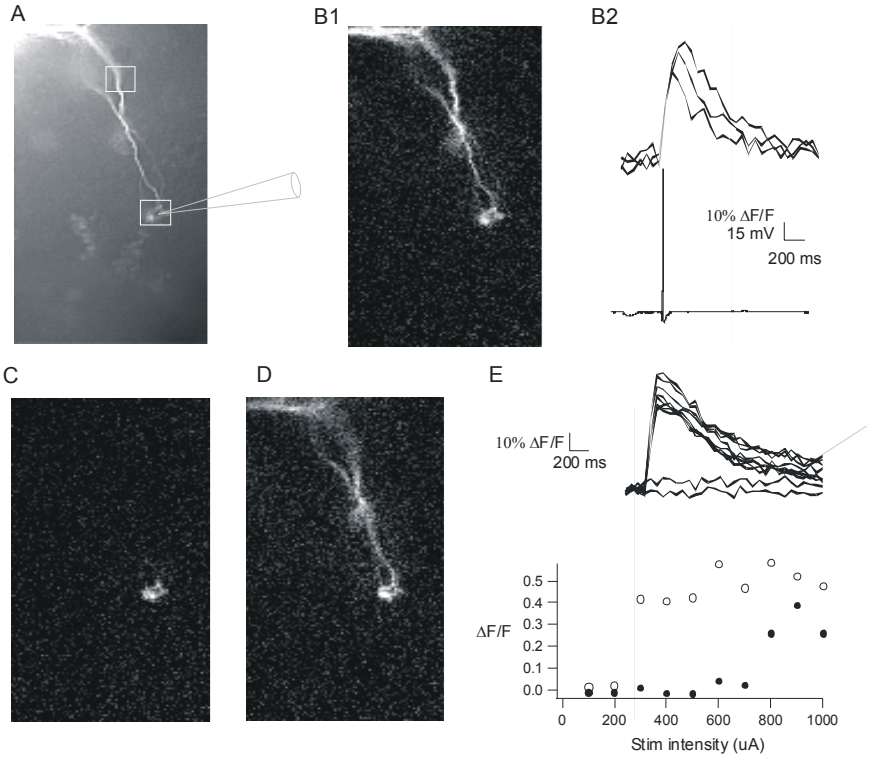

Figure 2: Isolated calcium transients in AOB mitral cell dendritic tufts. A) Fluorescence image showing a cell filled with calcium orange (100 uM). Boxes (35 um across) indicate the areas from which □F/F was measured for the traces in B2 and E. B) Action potential-evoked calcium transients. B1) Image shows a DF/F map for one 50 ms frame taken at the peak of an action-potential evoked calcium transient. B2, Top three traces show tuft calcium transients evoked by single action potentials elicited by somatic current injection. Bottom trace shows one of these action potentials. C, D) Maps of DF/F show the results of extracellular stimulation in the tuft. E) (Top) Traces showing the time course of the calcium elevation in the tuft for stimulation intensities ranging from 100-1000 uA. (Bottom) Peak of the calcium transient in the tuft (open circles) and in the proximal dendrite (filled circles) plotted against stimulation intensity. In DF/F maps, grey scale maps to 0-20% DF/F.

We next sought to determine whether the dendritic tufts of AOB mitral cells can support isolated dendritic spikes. That is, dendritic regenerative events that do not result in somatic action potentials. To look for isolated

calcium transients we filled mitral cells with fluorescent calcium dye and visualized their dendritic trees. After identifying a tuft we placed a glass stimulating electrode in the same glomerulus as the tuft, and used constant current pulses to stimulate the glomerulus. In a typical experiment (Figure 2 C, D, E), low intensity stimulation (0-200 μA) elicited no detectable calcium transient. Increasing stimulation intensity resulted in a calcium transient that was restricted to the dendritic tuft in the stimulated glomerulus (Figure 2 C). The amplitude of this isolated calcium event was similar to the amplitude of the action potential-evoked calcium transient in this cell. Further increasing stimulation intensity resulted in action potential firing and in calcium elevation throughout the primary dendrites and soma. These data suggest that all-or-none calcium events can be elicited in the tufts of AOB mitral cells. The fact that the calcium influx caused by these events is similar in magnitude to the calcium influx resulting from a backpropagating action potential suggests that these synaptically evoked calcium events are in fact isolated dendritic spikes.

Discussion

Here we describe an initial characterization of the properties of the dendritic trees of AOB mitral cells. We find that the morphology of these trees allows for electrical isolation of tufts from the soma and from each other, that these dendrites support robust backpropagation of action potentials and that isolated calcium spikes can be evoked in individual tufts. These observations suggest that dendrites of AOB mitral cells are likely to participate in the active integration of inputs to different AOB glomeruli.

Reference List

Bischofberger, J. & Jonas, P. (1997). Action potential propagation into the presynaptic dendrites of rat mitral cells. *J.Physiol* **504 (Pt 2)**, 359-365.

Chen, W. R., Midtgaard, J., & Shepherd, G. M. (1997). Forward and backward propagation of dendritic impulses and their synaptic control in mitral cells. *Science* **278**, 463-467.

Margrie, T. W., Sakmann, B., & Urban, N. N. (2001). Action potential propagation in mitral cell lateral dendrites is decremental and controls recurrent and lateral inhibition in the mammalian olfactory bulb. *Proc.Natl.Acad.Sci.U.S.A.* **98**, 319-324.

Meisami, E. & Bhatnagar, K. P. (1998). Structure and diversity in mammalian accessory olfactory bulb. *Microsc.Res.Tech.* **43**, 476-499.

Migliore, M. & Shepherd, G. M. (2002). Emerging rules for the distributions of active dendritic conductances. *Nat.Rev.Neurosci.* **3**, 362-370.

Nickell, W. T., Behbehani, M. M., & Shipley, M. T. (1994). Evidence for GABAB-mediated inhibition of transmission from the olfactory nerve to mitral cells in the rat olfactory bulb. *Brain Res.Bull.* **35**, 119-123.

Schaefer, A. T., Larkum, M. E., Sakmann, B., & Roth, A. (2003). Coincidence detection in pyramidal neurons is tuned by their dendritic branching pattern. *J.Neurophysiol.*

Segev, I. & Parnas, I. (1983). Synaptic integration mechanisms. Theoretical and experimental investigation of temporal postsynaptic interactions between excitatory and inhibitory inputs. *Biophys.J.* **41**, 41-50.

Shepherd, G. M., Brayton, R. K., Miller, J. P., Segev, I., Rinzel, J., & Rall, W. (1985). Signal enhancement in distal cortical dendrites by means of interactions between active dendritic spines. *Proc.Natl.Acad.Sci.U.S.A* **82**, 2192-2195.

Spruston, N., Jaffe, D. B., & Johnston, D. (1994). Dendritic attenuation of synaptic potentials and currents: the role of passive membrane properties. [Review]. *Trends in Neurosciences* **17**, 161-166.